'Hole Redistribution' Model Explaining the Thermally Activated R_{ON} Stress/Recovery Transients in Carbon-Doped AlGaN/GaN Power MIS-HEMTs

Nicolò Zagni, *Student Member, IEEE*, Alessandro Chini, Francesco Maria Puglisi, *Member, IEEE*, Matteo Meneghini, *Senior Member, IEEE*, Gaudenzio Meneghesso, *Fellow, IEEE*, Enrico Zanoni, *Fellow, IEEE*, Paolo Pavan, *Senior Member, IEEE*, and Giovanni Verzellesi, *Senior Member, IEEE*

***Abstract*—R_{ON} degradation due to stress in GaN-based power devices is a critical issue that limits, among other effects, long-term stable operation. Here, by means of two-dimensional device simulations, we show that the R_{ON} increase and decrease during stress and recovery experiments in Carbon-doped AlGaN/GaN power MIS-HEMTs can be explained with a model based on the emission, redistribution, and re-trapping of holes within the Carbon-doped buffer ('hole redistribution', in short). By comparing simulation results with front- and back-gate off-state stress experiments we provide an explanation for the puzzling observation of both stress and recovery transients being thermally activated with the same activation energy of about 0.9 eV. This finds a straightforward justification in a model in which both R_{ON} degradation and recovery processes are limited by hole emission by dominant Carbon-related acceptors that are energetically located at about 0.9 eV from the GaN valence band.**

***Index Terms*—GaN MIS-HEMT, Current Collapse, Off-State Stress, ON-Resistance Degradation, Hole Redistribution**

I. Introduction

POWER devices based on the AlGaN/GaN heterostructure are becoming a popular technology solution as a replacement for Silicon devices [1]. The High Electron Mobility Transistors (HEMTs) based on this semiconductor system exhibit enhanced switching speed and breakdown field capability, enabling operation at higher operating voltage/frequency/temperature [1], [2]. However, the introduction of AlGaN/GaN HEMTs into the mass market not only depends on the demonstration of outstanding performance but also on the stable and reliable operation of these devices.

Mitigation of the failure mechanisms to ensure long-term reliable operation is therefore crucial to the success of GaN power electronics. In this regard, several physical aspects related to the so-called current-collapse effect (dynamic drain current drop or on-resistance increase) and threshold voltage drift (influencing current-collapse as well) occurring when performing off-to-on (or on-to-off) switching still need to be fully understood. Experimentally, "stress" tests are carried out by applying bias conditions that are known to accelerate the so-called dynamic R_{ON} degradation, i.e. the increase in the device on-state resistance (R_{ON}) during the typical pulse-mode operation of power transistors in power switching converters.

In this work, we propose an explanation for the on-resistance (R_{ON}) behavior during both front- and back-gating OFF-state stress and recovery experiments reported for AlGaN/GaN Metal-Insulator-Semiconductor HEMTs (MIS-HEMTs) featuring a Carbon-doped buffer, which is based on a hole emission/redistribution/re-trapping model ('hole redistribution', in short). This paper is based on a recent conference paper of ours [3] where only back-gating stress/recovery were considered, and extends our analysis to more customary front-gating stress/recovery experiments.

Carbon (C) doping is a widespread technology solution to reduce buffer conductivity and increase breakdown voltage for power applications [4], [5]. The introduction of acceptor traps associated with C-doping, however, leads to an enhancement of current collapse and dynamic R_{ON} degradation during OFF-state stress [6]. It is widely accepted that this is due to negative charge build-up in the C-related traps within the buffer [7]–[11]. This phenomenon is conventionally attributed to electron capture into buffer traps [8]–[11]. The work by *Meneghesso et*

N. Zagni, A. Chini, F. M. Puglisi, and P. Pavan are with the Department of Engineering "Enzo Ferrari", Università di Modena e Reggio Emilia, 41125, Modena, Italy. (e-mail: nicolo.zagni@unimore.it).

M. Meneghini, G. Meneghesso, and E. Zanoni are with the Department of Information Engineering (DEI), University of Padova, 35131, Padova, Italy.

G. Verzellesi is with Department of Sciences and Methods for Engineering (DISMI) and EN&TECH Center, University of Modena and Reggio Emilia, 42122, Reggio Emilia, Italy.

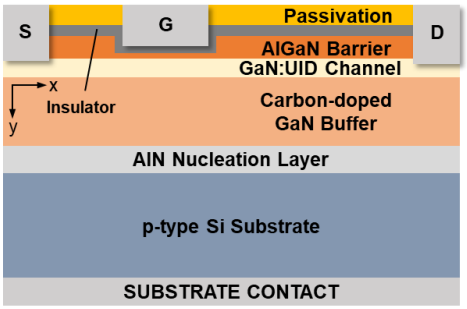

Fig. 1. Cross-section of the simulated MIS-HEMT with the recessed AlGaN barrier.

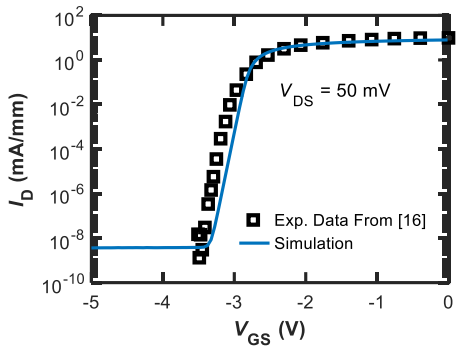

Fig. 2. Calibration of simulated (blue solid lines) against experimental data from [16] (black squares) I_D-V_{GS} characteristics.

al. in [7] reports on the R_{ON} stress and recovery behavior measured in power MIS-HEMTs during front- and back-gating experiments, finding that both transients under both test conditions are thermally activated with the *same* activation energy (E_A) of about 0.9 eV. In [7], a possible explanation for this was proposed, based on the observed correlation of the thermally activated stress with the increase with temperature of buffer leakage [8]. Moreover, the discharging of C-related buffer traps during recovery transients was also attributed to thermally activated vertical/lateral leakage paths in other works [6], [12], [13].

Here, we propose that the activation energy of both stress and recovery processes can be directly attributed to the dominant acceptor trap energy level associated with Carbon in the buffer, as a result of hole emission, redistribution, and re-trapping in the C-doped buffer. Stress is performed either: *i)* by applying a negative bias to the gate contact (V_G) and a large positive bias to the drain contact (V_D) (with source and substrate contacts grounded), or *ii)* by applying a negative bias to the substrate contact (V_B) (with all other contacts grounded). We will refer to the above stress conditions as to front- and back-gating OFF-state stress, respectively (FGOS/BGOS in short).

The proposed model: *i)* is seamlessly related to the commonly accepted model for C doping in GaN, i.e., a dominant acceptor trap level at about 0.9 eV from the valence band edge (E_V) [14], that turns the GaN buffer into a weakly p-type region; *ii)* does not require, though does not exclude, possible charging/discharging mechanism through leakage paths; *iii)* self-consistently captures the dynamics of stress/recovery processes up to drain bias for which C doping is able to effectively suppress electron leakage current through the GaN buffer, i.e., before significant electron injection into the buffer from the source and/or from the substrate takes place.

The paper is organized as follows. In Section II, the modeling framework is illustrated along with the analyzed device structure and the relevant physical models employed. Results are presented and discussed in Section III. Finally, conclusions are drawn in Section IV.

II. Modeling Framework

The structure employed in the simulations in this work is sketched in Fig. 1, resembling a typical power AlGaN/GaN MIS-HEMT. The two-dimensional (2D) numerical device simulations were carried out with SDevice™ (Synopsys Inc.) Technology CAD (TCAD) simulator [15]. We first calibrated our TCAD simulation deck against experimental I_D-V_{GS} data reported in [16]. The outcome is shown in Fig. 2. As reported in [17], the calibrated device features a highly-conductive p-type Si substrate, an AlN nucleation layer (200 nm), a C-doped GaN buffer (2.3 µm), an unintentionally doped (UID) GaN channel (150 nm), an $Al_{0.25}Ga_{0.75}N$ barrier (10 nm) and a Si_3N_4 passivation layer over the access regions (120 nm). The gate insulator consists of an Al_2O_3 layer (15 nm) that is added to the structure after partially recessing the barrier and leaving 3.7 nm of residual AlGaN under the gate [16]. The gate-to-drain access region is 5 µm [16] (while it is 10 µm in [8], [17] from which stress and recovery experimental data are taken).

Charge transport was modelled by means of the drift-diffusion model. The piezoelectric polarization at the heterointerfaces was included by using the default strain model of the simulator [15]. A fully dynamic trap modelling approach was adopted, with one Shockley-Read-Hall (SRH) trap-balance equation for each distinct trap level included, describing the dynamics of trap occupation without any quasi-static approximation. A detailed description of the modeling approach to describe device physics in AlGaN/GaN based HEMTs can be found in [18]. The gate insulator (Al_2O_3) is assumed ideal, i.e., gate leakage current is neglected.

C doping in the GaN buffer was modelled by considering a dominant deep acceptor trap at 0.9 eV above E_V partially compensated by a shallow donor trap at 0.11 eV below E_C [17]. To reproduce the experimental results, the adopted trap concentrations were 2×10^{18} cm^{-3} and 1×10^{18} cm^{-3}, for C-related acceptors and donors, respectively. This corresponds to an effective acceptor density of 1×10^{18} cm^{-3} with a compensation ratio of 50%. No additional traps were considered, while in all nitride layers an n-type doping density of $1x10^{15}$ cm^{-3} was assumed, as conventionally done when simulating GaN devices to account for the unintentional n-type conductivity due to shallow-donor impurities like Oxygen and Silicon during growth [5], [19].

The C doping model employed in this work was developed over the years by our group and allowed explaining measured current-collapse, threshold voltage shifts, and breakdown effects in different GaN power HEMTs [3], [20]–[25]. The dependability of the acceptor-donor model for C doping is further confirmed by its capability of reproducing source-drain leakage currents and off-state breakdown as reported in [19]. The key assumption in the adopted C doping model is that the dominant deep acceptor traps for holes are partially compensated by shallow donor traps for electrons. The actual energy position of donor traps however, if sufficiently shallow,

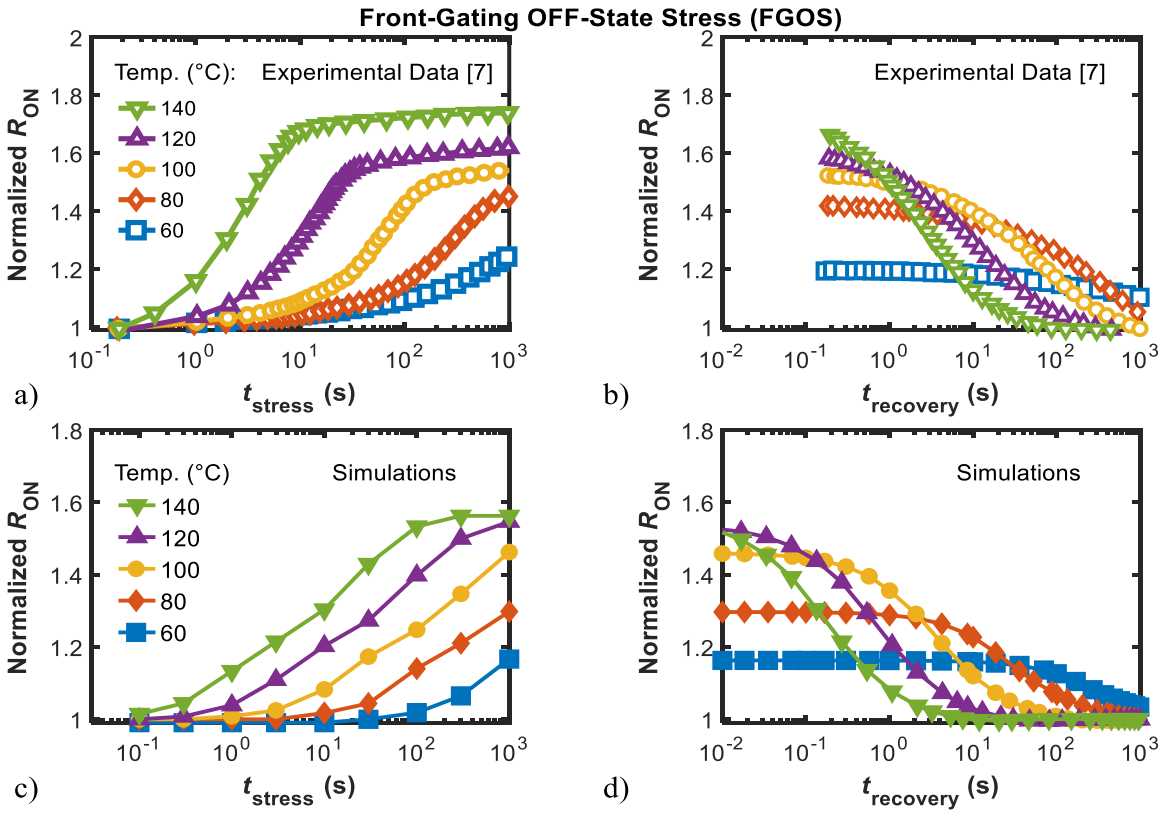

Fig. 3. R_{ON} variations (normalized w.r.t. the pre-stress value) during FGOS (a, c) and consequent recovery (b, d) experiments (from [7]) and simulations carried out at different temperatures (see legend). Stress/Recovery conditions are (V_G, V_D, V_B) = (-8, 25, 0) V, and (V_G, V_D, V_B) = (0, 0.5, 0) V, respectively.

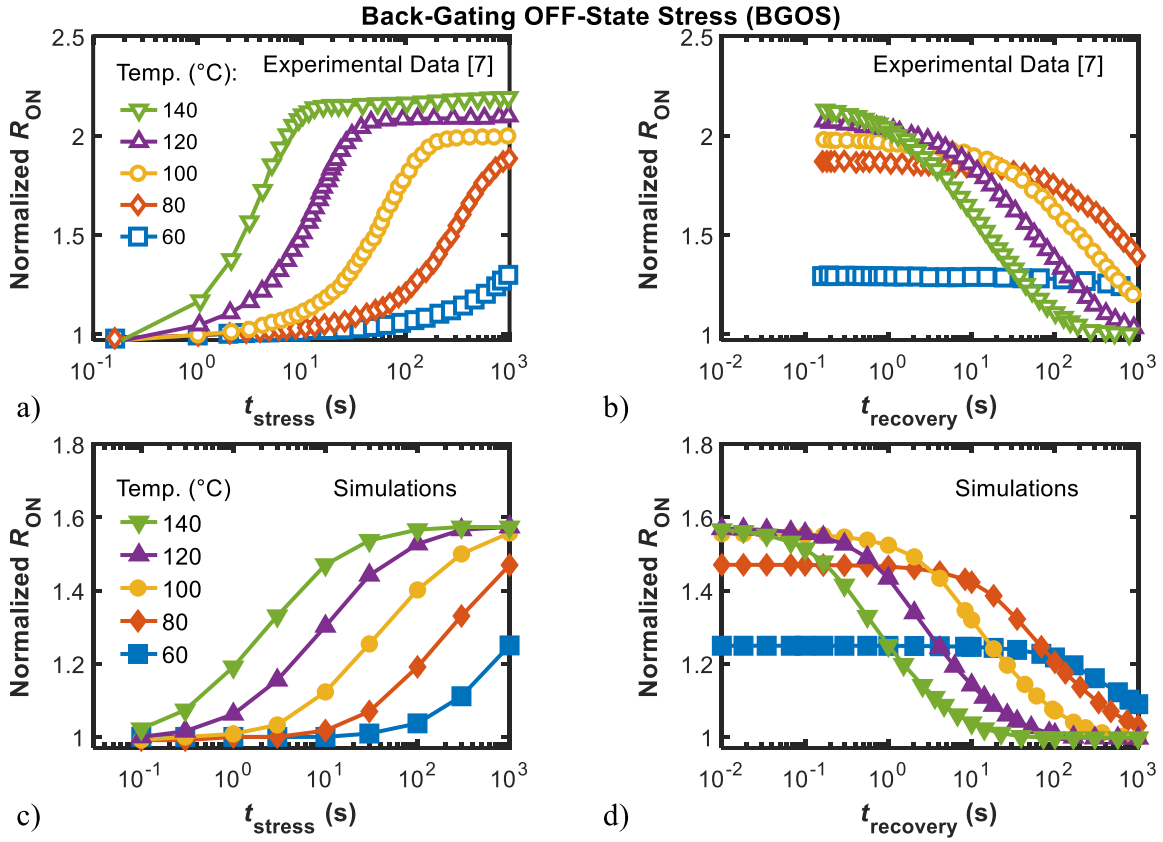

Fig. 4. R_{ON} variations (normalized w.r.t. the pre-stress value) during BGOS (a, c) and consequent recovery (b, d) experiments (from [7]) and simulations carried out at different temperatures (see legend). Stress/Recovery conditions are (V_G, V_D, V_B) = (0, 0, -25) V, and (V_G, V_D, V_B) = (0, 0.5, 0) V, respectively.

has little influence on simulation results. Indeed, C-related donors could actually be closer to E_C or even be modelled as completely ionized doping, in agreement with recent hybrid-functional DFT calculations [14], [26]. Further, an experimental indication that C doping introduces donors besides acceptors is found in [27]. According to previous reports, for moderate C doping concentration (i.e., $\leq 10^{18}$ cm^{-3}) it is appropriate to model dopants as discrete point defects, whereas for concentrations of about (or higher than) 10^{19} cm^{-3} it is more appropriate to use a defect-band model [28].

III. Results and Discussion

We will first compare simulation results with the experimental data obtained from stress and recovery tests carried out on the MIS-HEMT, as reported in [7]. The sketch of the cross-section is shown in Fig. 1. Both stress conditions (i.e., FGOS and BGOS) bias the device in the subthreshold region. However, the BGOS setup is useful to rule out surface trapping effects – which can be present during FGOS instead – thus allowing to attribute the observed phenomena to buffer traps only [29], [30]. Under BGOS tests in fact, the formed 2DEG channel screens the superficial layers from the field effect induced by back-gating, so surface effects should be negligible [29]. The fact that a similar kinetics was found for FGOS and BGOS is an indication that buffer traps are mainly involved [8]. Since we only include buffer traps in our simulation setup, both FGOS and BGOS conditions modify the state of C-related traps only. The comparison between experimental data and simulation results is shown in Figs. 3 and 4, with stress and recovery conditions applied as follows. *i*) FGOS and recovery: (V_G, V_D, V_B) = (-8, 25,0) V and (V_G, V_D, V_B) = (0, 0.5, 0) V, respectively; *ii*) BGOS and recovery: (V_G, V_D, V_B) = (0, 0, -25) V and (V_G, V_D, V_B) = (0, 0.5, 0) V, respectively. The chosen experimental FGOS and BGOS conditions represent "intermediate" OFF-state bias conditions, i.e., with drain voltages that are large enough to have appreciable dynamic R_{ON} effects but, at the same time, low enough not to promote significant electron injection through the C-doped buffer due to lateral source-drain punch-through or vertical leakage current. During stress simulations, R_{ON} values were obtained by fast sweeping the device bias to measurement conditions (V_G, V_D) = (0, 0.5) V in 10 ms to mimic on-the-fly (OTF) measurements [7]. During recovery, instead, R_{ON} was monitored throughout the simulation as recovery and measurement conditions were the same. R_{ON} results in Figs. 3 and 4 are normalized with respect to the fresh value at each temperature to purify results from the R_{ON} degradation induced by mobility reduction. Recovery tests were performed immediately after the stress phase was completed. Since R_{ON} measurement takes about 50 ms [7] no measurement data points were acquired for recovery time less than 100 ms. For both FGOS and BGOS, simulation results can reproduce reasonably well the essential features shown by the experimental results taken at different temperatures. That is, simulations capture the thermally activated processes at the basis of both R_{ON} degradation and recovery, as well as the time constant ranges.

As shown in [7], stress and recovery transients are found to be thermally activated with similar activation energies in the range 0.84-0.95 eV, irrespective of the stress condition. We report the experimental Arrhenius plots shown in [7] (for stress only) in Fig. 5 for both FGOS and BGOS conditions and compare them with simulation results (in this case showing both stress and recovery). The time constants at each temperature for both experiments and simulations were extracted by fitting the curves with the stretched exponential method [31]. The data at 60 °C were not suitable for the extraction of a time constant and were therefore excluded from the Arrhenius plot, the latter still having four reliable points for the extrapolation of E_A. As it can be noted, the Arrhenius signature of the stress process is well reproduced by our simulations and, more importantly, simulations predict the same activation energy of about 0.9 eV for both stress and recovery in either FGOS/BGOS conditions.

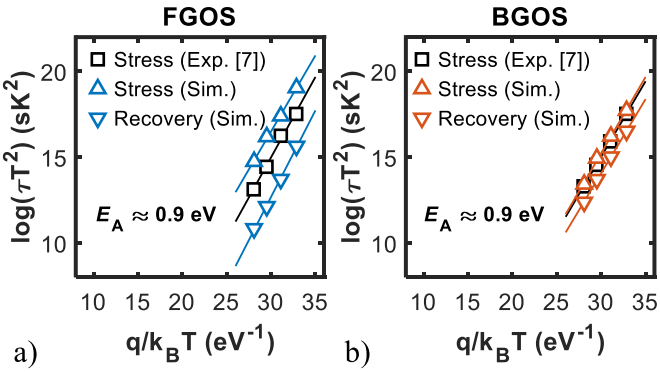

Fig. 5. Arrhenius plot for the simulated a) FGOS and b) BGOS transients as well as the relative recovery processes. Experimental data from [7] of stress processes are reported for comparison. Lines are the linear fitting of the data showing that both experiments and simulations are characterized by the same $E_A \approx 0.9$ eV.

Before providing the detailed explanation for this, it is important to observe that the R_{ON} increase shown in Figs. 3a) and 3c) (as well as in Figs. 4a) and 4c)) can in principle be induced by either electron trapping into or hole de-trapping from the buffer traps. Consequently, the corresponding R_{ON} recovery illustrated in Figs. 3b) and 3d) (as well as in Figs. 4b) and 4d)) can be ascribed to either electron de-trapping or hole trapping, respectively. However, regardless of the actual charge carriers involved, the fact that both emission and capture processes are thermally activated and, more importantly, *exhibit the same activation energy* is not trivial. In fact, while carrier emission is always a thermally activated process, carrier capture can only be thermally activated in traps that feature a capture barrier, although the associated activation energy is generally different (and smaller) than the emission one [8], [11]. In the case of the devices considered here, the extracted E_A (for both stress and recovery) correlates very well with the transition energy of the dominant acceptor level (C_N) related to Carbon in GaN [13].

We will now show that this behavior can be explained with a hole emission, redistribution, and re-trapping model. The model applies to both FGOS and BGOS. Thus, we focus only on the latter case for simplicity of data presentation, as under back-gating conditions the buffer is uniformly exposed to the backside bias and all internal quantities are characterized by an almost one-dimensional distribution (along the device depth direction). In the following, we will explain the processes occurring during stress and recovery with the aid of the plots of the net ionized acceptor trap density, ($N_A^- - N_D^+$), and of the

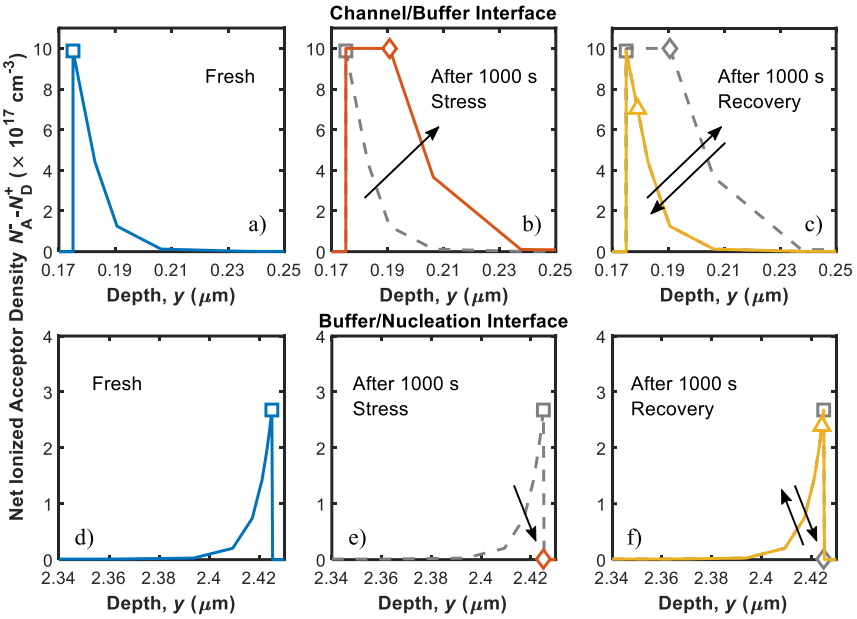

Fig.6. Net ionized acceptor trap density, $N_A^- - N_D^+$, along the vertical direction in the Gate-to-Drain access region at different conditions, namely: fresh (a, d), after 1000 s stress (b, e), and after 1000 s recovery (c, f) near the channel/buffer interface (a-c) and near the buffer/nucleation interface (d-f). BGOS conditions were applied (T = 100 °C).

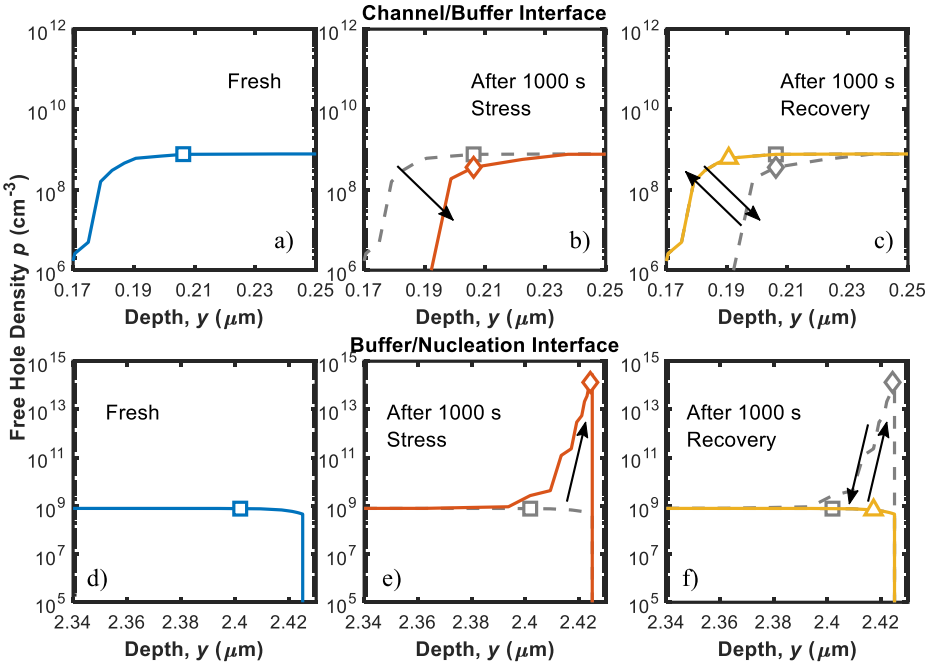

Fig. 7. Free hole density, p, along the vertical direction in the Gate-to-Drain access region at different conditions, namely: fresh (a, d), after 1000 s stress (b, e), and after 1000 s recovery (c, f) near the channel/buffer interface (a-c) and near the buffer/nucleation interface (d-f). BGOS conditions were applied (T = 100 °C).

free hole density, p, shown in Figs. 6 and 7. These plots are taken along a cutline parallel to the device depth drawn in the middle of the gate-to-drain access region and zoomed in at the top and bottom regions of the buffer, i.e., at the channel/buffer and nucleation/buffer interface, respectively. Note that the ionized donor trap density in the buffer remains constant (not shown) because the energy level of these traps is shallow (i.e., 0.11 eV from E_C) [19]. The C-doped buffer behaves as a weakly p-type region and the C-related donors simply have the role of partially compensating the dominant acceptor levels, without causing dynamic effects themselves. This picture can change at higher voltages than those considered here, as approaching lateral or vertical breakdown conditions significant electron injection into the C-doped buffer can take place either from the source or the substrate, respectively. Under such conditions, transport processes may impact the stress/recovery kinetics, as suggested in [32].

During stress, $(N_A^- - N_D^+)$ (net negative charge) in the top region of the buffer close to the channel increases because holes are being emitted from the 0.9-eV C-related acceptor traps to the valence band. This correlates with the observed R_{ON} increase during stress. The variation in $(N_A^- - N_D^+)$ close to the channel is evident by comparing the cases before and after stress in Figs. 6a) and 6b). The hole emission process is

thermally activated with 0.9-eV activation energy, see Fig. 5b). The holes being emitted at the top region of the buffer (compare Figs. 7a) and 7b)), drift towards the bottom edge of the buffer attracted by the negative V_B (in this case, -25 V), and accumulate at the buffer/nucleation layer interface, compare Figs. 7d) and 7e). The free holes get partially trapped and thus discharge the negatively charged acceptor traps at the same interface, compare Figs. 6d) and 6e). During recovery, all processes described above are inverted. Holes are emitted from C-related acceptors in the bottom region of the buffer, see Fig. 7f), and drift back towards the channel/buffer interface, see Fig. 7c), where they get re-trapped by the acceptor states from which they were emitted during stress. This process decreases $(N_A^- - N_D^+)$ at the channel/buffer interface as shown in Fig. 6c), thus explaining the R_{ON} decrease during recovery. The hole re-trapping process during recovery is also thermally activated with a 0.9-eV energy, since the re-trapped holes in the upper part of the buffer need to be emitted from the C-related acceptor traps in the bottom region of the buffer, see Fig. 6f). After 1000 s of recovery, the state prior to stress is fully restored (as testified by the results in Fig. 4) and consequently the *p* peak at the bottom of the buffer disappears, see Fig. 7f). The recovery phase fully restores the pre-stress value of R_{ON} because the holes emitted during stress do not leak out from the device contacts or recombine with electrons. This is further confirmed by the fact that while $(N_A^- - N_D^+)$ varies locally in the buffer, as shown in Fig. 6, its integral value in the buffer stays constant. For instance, $\int (N_A^- - N_D^+) dxdy \approx 1.6 \times 10^{17}$ cm^{-3}µm^2 (at T = 100 °C) prior to and after the stress phase and after the recovery one.

IV. Conclusions

We presented a 'hole redistribution' model explaining the R_{ON} stress/recovery experiments in C-doped AlGaN/GaN power MIS-HEMTs. Stress is ascribed to hole emission from C-related acceptor traps close to the channel/buffer interface that redistribute and get trapped in the same type of traps in the bottom region of the buffer close to the buffer/nucleation interface. During recovery, the opposite process takes place: the previously trapped holes in the bottom part of the buffer are emitted and get re-trapped by the same traps at the top of the buffer that emitted them during stress. The proposed model: 1) solves the puzzle of the activation energy being the same in both stress/recovery phases, and 2) explains the full recovery of the R_{ON} after the complete stress-and-recovery cycle in the analyzed devices.

Acknowledgment

The authors would like to thank Dr. Ferdinando Iucolano for fruitful discussion.

References

[1] H. Amano, Y. Baines, E. Beam, M. Borga, T. Bouchet, P. R. Chalker, M. Charles, K. J. Chen, N. Chowdhury, R. Chu, C. De Santi, M. M. De Souza, S. Decoutere, L. Di Cioccio, B. Eckardt, T. Egawa, P. Fay, J. J. Freedsman, L. Guido, O. Häberlen, G. Haynes, T. Heckel, D. Hemakumara, P. Houston, J. Hu, M. Hua, Q. Huang, A. Huang, S. Jiang, H. Kawai, D. Kinzer, M. Kuball, A. Kumar, K. B. Lee, X. Li, D. Marcon, M. März, R. McCarthy, G. Meneghesso, M. Meneghini, E. Morvan, A. Nakajima, E. M. S. Narayanan, S. Oliver, T. Palacios, D. Piedra, M. Plissonnier, R. Reddy, M. Sun, I. Thayne, A. Torres, N. Trivellin, V. Unni, M. J. Uren, M. Van Hove, D. J. Wallis, J. Wang, J. Xie, S. Yagi, S. Yang, C. Youtsey, R. Yu, E. Zanoni, S. Zeltner, and Y. Zhang, "The 2018 GaN power electronics roadmap," *J. Phys. D. Appl. Phys.*, vol. 51, no. 16, p. 163001, 2018. DOI: 10.1088/1361-6463/aaaf9d.

[2] J. A. del Alamo and E. S. Lee, "Stability and Reliability of Lateral GaN Power Field-Effect Transistors," *IEEE Trans. Electron Devices*, vol. 66, no. 11, pp. 4578–4590, Nov. 2019. DOI: 10.1109/TED.2019.2931718.

[3] N. Zagni, A. Chini, F. M. Puglisi, P. Pavan, M. Meneghini, G. Meneghesso, E. Zanoni, and G. Verzellesi, "Trap Dynamics Model Explaining the R ON Stress/Recovery Behavior in Carbon-Doped Power AlGaN/GaN MOS-HEMTs," in *2020 IEEE International Reliability Physics Symposium (IRPS)*, Apr. 2020, pp. 1–5. DOI: 10.1109/IRPS45951.2020.9128816.

[4] E. Bahat-Treidel, F. Brunner, O. Hilt, E. Cho, J. Würfl, and G. Trankle, "AlGaN/GaN/GaN:C back-barrier HFETs with breakdown voltage of over 1 kV and low RON× A," *IEEE Trans. Electron Devices*, vol. 57, no. 11, pp. 3050–3058, Nov. 2010. DOI: 10.1109/TED.2010.2069566.

[5] M. J. Uren, J. Moreke, and M. Kuball, "Buffer design to minimize current collapse in GaN/AlGaN HFETs," *IEEE Trans. Electron Devices*, vol. 59, no. 12, pp. 3327–3333, 2012. DOI: 10.1109/TED.2012.2216535.

[6] M. J. Uren, S. Karboyan, I. Chatterjee, A. Pooth, P. Moens, A. Banerjee, and M. Kuball, "'Leaky Dielectric' Model for the Suppression of Dynamic RON in Carbon-Doped AlGaN/GaN HEMTs," *IEEE Trans. Electron Devices*, vol. 64, no. 7, pp. 2826–2834, Jul. 2017. DOI: 10.1109/TED.2017.2706090.

[7] G. Meneghesso, M. Meneghini, I. Rossetto, D. Bisi, S. Stoffels, M. Van Hove, S. Decoutere, and E. Zanoni, "Reliability and parasitic issues in GaN-based power HEMTs: a review," *Semicond. Sci. Technol.*, vol. 31, no. 9, p. 093004, Sep. 2016. DOI: 10.1088/0268-1242/31/9/093004.

[8] D. Bisi, M. Meneghini, F. A. Marino, D. Marcon, S. Stoffels, M. Van Hove, S. Decoutere, G. Meneghesso, and E. Zanoni, "Kinetics of Buffer-Related R_{ON}-Increase in GaN-on-Silicon MIS-HEMTs," *IEEE Electron Device Lett.*, vol. 35, no. 10, pp. 1004–1006, Oct. 2014. DOI: 10.1109/LED.2014.2344439.

[9] E. Fabris, M. Meneghini, C. De Santi, M. Borga, G. Meneghesso, E. Zanoni, Y. Kinoshita, K. Tanaka, H. Ishida, and T. Ueda, "Hot-Electron Effects in GaN GITs and HD-GITs: A Comprehensive Analysis," in *IEEE International Reliability Physics Symposium Proceedings*, May 2019, pp. 1–6. DOI: 10.1109/IRPS.2019.8720472.

[10] P. Moens, P. Vanmeerbeek, A. Banerjee, J. Guo, C. Liu, P. Coppens, A. Salih, M. Tack, M. Caesar, M. J. Uren, M. Kuball, M. Meneghini, G. Meneghesso, and E. Zanoni, "On the impact of carbon-doping on the dynamic Ron and off-state leakage current of 650V GaN power devices," *Proc. Int. Symp. Power Semicond. Devices ICs*, vol. 2015-June, pp. 37–40, 2015. DOI: 10.1109/ISPSD.2015.7123383.

[11] K. Tanaka, M. Ishida, T. Ueda, and T. Tanaka, "Effects of Deep Trapping States at High Temperatures on Transient Performance of AlGaN/GaN Heterostructure Field-Effect Transistors," *Jpn. J. Appl. Phys.*, vol. 52, no. 4S, p. 04CF07, Apr. 2013. DOI: 10.7567/JJAP.52.04CF07.

[12] P. Moens, A. Banerjee, M. J. Uren, M. Meneghini, S. Karboyan, I. Chatterjee, P. Vanmeerbeek, M. Cäsar, C. Liu, A. Salih, E. Zanoni, G. Meneghesso, M. Kuball, M. Tack, M. Casar, C. Liu, A. Salih, E. Zanoni, G. Meneghesso, M. Kuball, and M. Tack, "Impact of buffer leakage on intrinsic reliability of 650V AlGaN/GaN HEMTs," in *Proceedings of the IEEE International Electron Devices Meeting (IEDM)*, Dec. 2015, vol. 2016-Febru, pp. 35.2.1-35.2.4. DOI: 10.1109/IEDM.2015.749831.

[13] M. Meneghini, A. Tajalli, P. Moens, A. Banerjee, E. Zanoni, and G. Meneghesso, "Trapping phenomena and degradation mechanisms in GaN-based power HEMTs," *Mater. Sci. Semicond. Process.*, vol. 78, pp. 118–126, May 2018. DOI: 10.1016/j.mssp.2017.10.009.

[14] J. L. Lyons, A. Janotti, and C. G. Van De Walle, "Effects of carbon on the electrical and optical properties of InN, GaN, and AlN," *Phys. Rev. B - Condens. Matter Mater. Phys.*, vol. 89, no. 3, pp. 1–8, Jan. 2014. DOI: 10.1103/PhysRevB.89.035204.

[15] Synopsys, "Sentaurus SDevice Manual (N-2017.09)." 2017.

[16] G. Meneghesso, M. Meneghini, D. Bisi, I. Rossetto, T. L. Wu, M. Van Hove, D. Marcon, S. Stoffels, S. Decoutere, and E. Zanoni, "Trapping and reliability issues in GaN-based MIS HEMTs with partially recessed gate," *Microelectron. Reliab.*, vol. 58, pp. 151–157, 2016. DOI: 10.1016/j.microrel.2015.11.024.

[17] A. Armstrong, C. Poblenz, D. S. Green, U. K. Mishra, J. S. Speck, and S. A. Ringel, "Impact of substrate temperature on the incorporation of carbon-related defects and mechanism for semi-insulating behavior in GaN grown by molecular beam epitaxy," *Appl. Phys. Lett.*, vol. 88, no. 8, pp. 1–4, Feb. 2006. DOI: 10.1063/1.2179375.

[18] V. Joshi, A. Soni, S. P. Tiwari, and M. Shrivastava, "A Comprehensive Computational Modeling Approach for AlGaN/GaN HEMTs," *IEEE Trans. Nanotechnol.*, vol. 15, no. 6, pp. 947–955, Nov. 2016. DOI: 10.1109/TNANO.2016.2615645.

[19] V. Joshi, S. P. Tiwari, and M. Shrivastava, "Part I: Physical Insight into Carbon-Doping-Induced Delayed Avalanche Action in GaN Buffer in AlGaN/GaN HEMTs," *IEEE Trans. Electron Devices*, vol. 66, no. 1, pp. 561–569, 2019. DOI: 10.1109/TED.2018.2878770.

[20] G. Verzellesi, L. Morassi, G. Meneghesso, M. Meneghini, E. Zanoni, G. Pozzovivo, S. Lavanga, T. Detzel, O. Häberlen, and G. Curatola, "Influence of buffer carbon doping on pulse and AC behavior of insulated-gate field-plated power AlGaN/GaN HEMTs," *IEEE Electron Device Lett.*, vol. 35, no. 4, pp. 443–445, 2014. DOI: 10.1109/LED.2014.2304680.

[21] G. Meneghesso, R. Silvestri, M. Meneghini, A. Cester, E. Zanoni, G. Verzellesi, G. Pozzovivo, S. Lavanga, T. Detzel, O. Haberlen, and G. Curatola, "Threshold voltage instabilities in D-mode GaN HEMTs for power switching applications," *IEEE Int. Reliab. Phys. Symp. Proc.*, pp. 6–10, 2014. DOI: 10.1109/IRPS.2014.6861109.

[22] A. Chini, G. Meneghesso, M. Meneghini, F. Fantini, G. Verzellesi, A. Patti, and F. Iucolano, "Experimental and Numerical Analysis of Hole Emission Process from Carbon-Related Traps in GaN Buffer Layers," *IEEE Trans. Electron Devices*, vol. 63, no. 9, pp. 3473–3478, Sep. 2016. DOI: 10.1109/TED.2016.2593791.

[23] N. Zagni, F. M. Puglisi, P. Pavan, A. Chini, and G. Verzellesi, "Insights into the off-state breakdown mechanisms in power GaN HEMTs," *Microelectron. Reliab.*, vol. 100–101, p. 113374, Sep. 2019. DOI: 10.1016/j.microrel.2019.06.066.

[24] N. Zagni, A. Chini, F. M. Puglisi, P. Pavan, and G. Verzellesi, "The Role of Carbon Doping on Breakdown, Current Collapse, and Dynamic On-Resistance Recovery in AlGaN/GaN High Electron Mobility Transistors on Semi-Insulating SiC Substrates," *Phys. status solidi*, vol. 217, p. 1900762, Dec. 2019. DOI: 10.1002/pssa.201900762.

[25] N. Zagni, A. Chini, F. M. Puglisi, P. Pavan, and G. Verzellesi, "The effects of carbon on the bidirectional threshold voltage instabilities induced by negative gate bias stress in GaN MIS-HEMTs," *J. Comput. Electron.*, vol. 19, no. 4, pp. 1555–1563, Dec. 2020. DOI: 10.1007/s10825-020-01573-8.

[26] M. Matsubara and E. Bellotti, "A first-principles study of carbon-related energy levels in GaN. I. Complexes formed by substitutional/interstitial carbons and gallium/nitrogen vacancies," *J. Appl. Phys.*, vol. 121, no. 19, p. 195701, May 2017. DOI: 10.1063/1.4983452.

[27] A. Fariza, A. Lesnik, J. Bläsing, M. P. Hoffmann, F. Hörich, P. Veit, H. Witte, A. Dadgar, and A. Strittmatter, "On reduction of current leakage in GaN by carbon-doping," *Appl. Phys. Lett.*, vol. 109, no. 21, p. 212102, 2016. DOI: 10.1063/1.4968823.

[28] C. Koller, G. Pobegen, C. Ostermaier, and D. Pogany, "Effect of Carbon Doping on Charging/Discharging Dynamics and Leakage Behavior of Carbon-Doped GaN," *IEEE Trans. Electron Devices*, vol. 65, no. 12, pp. 5314–5321, 2018. DOI: 10.1109/TED.2018.2872552.

[29] D. Bisi, M. Meneghini, M. Van Hove, D. Marcon, S. Stoffels, T.-L. L. Wu, S. Decoutere, G. Meneghesso, and E. Zanoni, "Trapping mechanisms in GaN-based MIS-HEMTs grown on silicon substrate," *Phys. status solidi*, vol. 212, no. 5, pp. 1122–1129, May 2015. DOI: 10.1002/pssa.201431744.

[30] S. Yang, C. Zhou, Q. Jiang, J. Lu, B. Huang, and K. J. Chen, "Investigation of buffer traps in AlGaN/GaN-on-Si devices by thermally stimulated current spectroscopy and back-gating measurement," *Appl. Phys. Lett.*, vol. 104, no. 1, p. 013504, Jan. 2014. DOI: 10.1063/1.4861116.

[31] D. Bisi, M. Meneghini, C. De Santi, A. Chini, M. Dammann, P. Bruckner, M. Mikulla, G. Meneghesso, and E. Zanoni, "Deep-level characterization in GaN HEMTs-Part I: Advantages and limitations of drain current transient measurements," *IEEE Trans. Electron Devices*, vol. 60, no. 10, pp. 3166–3175, 2013. DOI: 10.1109/TED.2013.2279021.

[32] F. Wach, M. J. Uren, B. Bakeroot, M. Zhao, S. Decoutere, and M. Kuball, "Low Field Vertical Charge Transport in the Channel and Buffer Layers of GaN-on-Si High Electron Mobility Transistors," *IEEE Electron Device Lett.*, 2020. DOI: 10.1109/LED.2020.3030341.